

# On Maximum Entropy Linear Feature Inversion

Paul M Baggenstoss *Fraunhofer FKIE*  
 Fraunhoferstraße 20, 53343 Wachtberg, Germany  
 p.m.baggenstoss@ieee.org

**Index Terms**—linear feature inversion, maximum entropy

**Abstract**—We revisit the classical problem of inverting dimension-reducing linear mappings using the maximum entropy (MaxEnt) criterion. In the literature, solutions are problem-dependent, inconsistent, and use different entropy measures. We propose a new unified approach that not only specializes to the existing approaches, but offers solutions to new cases, such as when data values are constrained to  $[0, 1]$ , which has new applications in machine learning.

## I. INTRODUCTION

### A. Problem Statement

Let  $\mathbf{x} \in \mathbb{X} \subset \mathbb{R}^N$  be an unknown input data sample. Let

$$\mathbf{z} = \mathbf{W}^T \mathbf{x}, \quad (1)$$

where  $\mathbf{W}$  is a full-rank  $N \times M$  matrix and  $M < N$ . Given  $\mathbf{z}$ , we wish to reconstruct  $\mathbf{x}$  by selecting a member of the set

$$\mathcal{M}(\mathbf{z}) = \{\mathbf{x} : \mathbf{W}^T \mathbf{x} = \mathbf{z}\}, \quad \mathbf{x} \in \mathbb{X}, \quad (2)$$

the set of all samples  $\mathbf{x} \in \mathbb{X}$  that reproduce the  $\mathbf{z}$ . Since  $\mathcal{M}(\mathbf{z})$  has an infinity of members, we must select a member based on some regularization criterion. The leading criterion is maximum entropy (MaxEnt), which is justified base on first principles [1]–[5], and can be seen as a general flatness measure [4]. Below, we revisit this classical problem, unify existing methods, and extend the solution to new data ranges  $\mathbb{X}$ , which have modern applications. We assume that the input data is not available, precluding machine learning approaches requiring training data pairs  $\{\mathbf{x}, \mathbf{z}\}$ .

### B. Maximum Entropy Approaches

MaxEnt linear feature inversion has been used in applications including image reconstruction [6]–[10], where (1) represents the point-spread function of the optics, and in *power spectral estimation*, where  $\mathbf{W}$  computes the auto-correlation function (ACF) [11]. There are at least two approaches, depending on if  $\mathbf{x}$  is seen as a probability distribution, or as a power spectrum [7], [12]. The MaxEnt principle [1], [2] holds that the data distribution should be selected to maximize uncertainty, measured by the distribution entropy

$$H_d = -\mathcal{E}_{\mathbf{x}} \{\log p(\mathbf{x})\} = -\int_{\mathbb{X}} \log p(\mathbf{x}) p(\mathbf{x}) d\mathbf{x}. \quad (3)$$

While the uniform distribution has the highest entropy on a fixed interval, other distributions arise if constraints are

imposed. Constraining variance results in the Gaussian distribution, and constraining the mean for positive-valued data results in the exponential distribution [13].

When  $\mathbf{x}$  is seen as a probability distribution, (3) is applied directly to  $\mathbf{x}$  in the discrete form [6], [8], [9], [12], [14]  $H_{ds}(\mathbf{x}) = -\sum_{i=1}^N x_i \log x_i$ , where  $\sum_{i=1}^N x_i = 1$ , however, is justified only for strictly positive-valued  $\mathbf{x}$ . If  $\mathbf{x}$  is seen as a power spectrum, spectral entropy

$$H_s(\mathbf{x}) = \sum_{i=1}^N \log x_i \quad (4)$$

is used, where  $\mathbf{W}$  computes the ACF. Maximizing the spectral entropy maximizes the entropy rate of a stationary process specified by the power spectrum  $\mathbf{x}$  [5], [10], [15], [16]. Spectral entropy is also used in image reconstruction [12], [17].

Although both distribution entropy and spectral entropy can be seen as general smoothness measures [7], [12], a unified treatment that has place for both would be desirable. Secondly, as far as we know, prior work on MaxEnt feature inversion has been applied to positive-valued data, but not to data bounded to other ranges, such as the finite interval  $[0, 1]$ .

In this paper, we present an approach that can be used with different combinations of data range and constraints. While classical MaxEnt feature inversion uses just one combination: positive-valued data with an implicit constraint on the mean and exponential prior distribution, we provide a table listing five combinations, all of which are solved by the same universal set of equations.

## II. IDEALIZED APPROACH

Our approach consists of two parts, an *idealized approach* which cannot be tractably solved, and an *asymptotic approach*, which has a closed-form solution and is asymptotically the same (as  $N$  becomes large) as the idealized approach.

### A. Main Idea

In the idealized approach, we propose a MaxEnt probability distribution on the set  $\mathcal{M}(\mathbf{z})$ , then let the mean of this distribution be the MaxEnt solution to the feature inversion problem. This can be justified because the mean can be seen as a smoothing operation applied to an infinite number of samples from the distribution, desirable from a regularization argument. Additionally, notice that  $\mathcal{M}(\mathbf{z})$  is the intersection of a linear subspace and  $\mathbb{X}$ , which is convex if  $\mathbb{X}$  is convex. The mean of the MaxEnt distribution will be the center of gravity on a convex set, far from the boundaries, avoiding artifacts caused when data “touches” the boundaries.

This work was supported jointly by the Office of Naval Research Global and the Defense Advanced Research Projects Agency under Research Grant - N62909-21-1-2024

## B. Mathematical Details

We first assume a MaxEnt prior distribution on  $\mathbb{X}$ , written  $p_{x,0}(\mathbf{x})$ . Prior to observing  $\mathbf{z}$ , all we know is that  $\mathbf{x}$  is contained in  $\mathbb{X}$ . The conditional distribution (given  $\mathbf{z}$ ) under the given prior, is written  $p_{x,0}(\mathbf{x}|\mathbf{z})$ , has support only on  $\mathcal{M}(\mathbf{z})$  and takes its shape from  $p_{x,0}(\mathbf{x})$ . It can be represented by

$$p_{x,0}(\mathbf{x}|\mathbf{z}) = \frac{1}{Z} \delta(\mathbf{z} - \mathbf{W}^T \mathbf{x}) p_{x,0}(\mathbf{x}), \quad (5)$$

where  $\delta$  is either a Dirac delta function, or an indicator function (equal to 1 if the argument is 0), depending on how it is used, and  $Z$  is a normalizing factor. As an aside, it can be shown [18] that  $Z = p_{x,0}(\mathbf{z})$ , which is  $p_{x,0}(\mathbf{x})$  mapped to the output of transformation (1)<sup>1</sup>.

As a MaxEnt solution, we propose to use the conditional mean of  $\mathbf{x}$  given  $\mathbf{z}$  under the given prior  $p_{x,0}(\mathbf{x})$

$$\bar{\mathbf{x}}_{\mathbf{z}} = \int_{\mathbf{x} \in \mathcal{M}(\mathbf{z})} \mathbf{x} p_{x,0}(\mathbf{x}|\mathbf{z}) d\mathbf{x}, \quad (6)$$

which is the weighted center of mass of the set  $\mathcal{M}(\mathbf{z})$ , weighted by  $p_{x,0}(\mathbf{x})$ . Since  $\mathcal{M}(\mathbf{z})$  is bounded by  $\mathbb{X}$ , the solution becomes intractable except in the case where  $\mathbb{X} = \mathbb{R}^N$ .

## C. Data Ranges and Prior Distributions

We consider three canonical data ranges that are common:

- $\mathbb{R}^N$  : Unbounded data,  $x_i \in (-\infty, \infty), \forall i$ .
- $\mathbb{P}^N$  : Positive-valued data,  $x_i \in [0, \infty), \forall i$ .
- $\mathbb{U}^N$  : Doubly bounded data,  $x_i \in [0, 1], \forall i$ .

In Table I, we list five useful combinations of data range  $\mathbb{X}$  and MaxEnt prior  $p_{0,x}(\mathbf{x})$ . Except in  $\mathbb{U}^N$ , the entropy of a distribution can go to infinity, so it is necessary to place constraints on the distribution, either fixed variance (Gaussian or truncated Gaussian) or fixed mean (exponential). For the chi-squared distribution with one degree of freedom, written Chi-sq(1), the mean as well as the mean of  $\log x$  is constrained.

TABLE I  
MAXENT PRIORS AND ACTIVATION FUNCTIONS. TG="TRUNCATED GAUSSIAN". TED="TRUNCATED EXPONENTIAL DISTRIBUTION".  
 $\mathcal{N}(x) \triangleq \frac{e^{-x^2/2}}{\sqrt{2\pi}}$  AND  $\Phi(x) \triangleq \int_{u=-\infty}^x \mathcal{N}(u) du$ .

$\mathbb{X}$	MaxEnt Prior		Activation	
	$p_{0,x}(\mathbf{x})$	Name	$\lambda(\alpha)$	Name
$\mathbb{R}^N$	$\prod_{i=1}^N \mathcal{N}(x_i)$	Gaussian	$\alpha$	linear
$\mathbb{P}^N$	$\prod_{i=1}^N 2\mathcal{N}(x_i)$	Trunc. Gauss.	$\alpha + \frac{\mathcal{N}(\alpha)}{\Phi(\alpha)}$	TG
$\mathbb{P}^N$	$\prod_{i=1}^N e^{-x_i}$	Expon.	$\frac{1}{1-\alpha}, \alpha < 1$	Expon.
$\mathbb{P}^N$	$\prod_{i=1}^N \frac{e^{-x_i/2}}{\sqrt{2\pi x}}$	Chi-sq.(1)	$\frac{1}{1-2\alpha}, \alpha < .5$	Ch.Sq(1)
$\mathbb{U}^N$	1	Uniform	$\frac{e^\alpha}{e^\alpha - 1} - \frac{1}{\alpha}$	TED

## D. Unified Exponential form of Prior distribution

It is well known that MaxEnt priors for moment constraints are of the exponential class [13]. For the priors in Table I, we

<sup>1</sup>In our notation, the argument of the distribution defines its region of support, and the subscript defines the space where it was defined. For example,  $p_{x,0}(\mathbf{z})$  is the image of a distribution defined on  $\mathbb{X}$ , but has support on the range of  $\mathbf{z}$ .

can restrict ourselves to the distribution class consisting of  $N$  independent random variables

$$p_s(\mathbf{x}; \boldsymbol{\alpha}, \alpha_0, \beta, \gamma) = \prod_{i=1}^N p_e(x_i; \alpha_i, \alpha_0, \beta, \gamma), \quad (7)$$

where  $p_e(x; \alpha, \alpha_0, \beta, \gamma)$  is a univariate distribution of the following exponential class

$$p_e(x; \alpha, \alpha_0, \beta, \gamma) = \frac{x^\gamma e^{(\alpha_0 + \alpha)x + \beta x^2}}{Z(\alpha, \alpha_0, \beta, \gamma)}, \quad (8)$$

where  $\boldsymbol{\alpha} = \{\alpha_1, \dots, \alpha_N\}$ . The MaxEnt prior is then written for  $\boldsymbol{\alpha} = \mathbf{0}$ ,

$$p_{0,x}(\mathbf{x}) = p_s(\mathbf{x}; \mathbf{0}, \alpha_0, \beta, \gamma). \quad (9)$$

In Table II the specific values of  $\alpha_0$ ,  $\beta$ , and  $\gamma$  are shown for different data ranges  $\mathbb{X}$  and moment assumptions, resulting in five different prior distributions.

TABLE II  
EXTENSION OF TABLE I SHOWING  $\alpha_0, \beta, \gamma$ , AND  $p_e(x; \alpha, \alpha_0, \beta, \gamma)$ . KEY: "TR." = TRUNCATED, "G" = GAUSSIAN, "EX." = EXPONENTIAL

$\mathbb{X}$	$\alpha_0$	$\beta$	$\gamma$	$p_e(x; \alpha, \alpha_0, \beta, \gamma)$	Name
$\mathbb{R}^N$	0	-.5	0	$\mathcal{N}(x - \alpha)$	Gaussian.
$\mathbb{P}^N$	0	-.5	0	$2\mathcal{N}(x - \alpha)$	Tr. G. (TG)
$\mathbb{P}^N$	-1	0	0	$(1 - \alpha)e^{-(1-\alpha)x}$	Expon.
$\mathbb{P}^N$	-.5	0	-.5	$\frac{1}{\sqrt{2\pi x(1-2\alpha)}} e^{-\frac{(1-2\alpha)x}{2}}$	Chi-Squared(1)
$\mathbb{U}^N$	0	0	0	$\left(\frac{\alpha}{e^\alpha - 1}\right) e^{\alpha x}$	Tr. Ex. (TED)

By comparing Tables I and II, it can be seen that the MaxEnt priors and activation functions given in Table I are special cases of  $p_s(\mathbf{x}; \boldsymbol{\alpha}, \alpha_0, \beta, \gamma)$  where  $\boldsymbol{\alpha} = \mathbf{0}$ .

## III. ASYMPTOTIC APPROACH

### A. Main Idea

The following closed form approximation to (6) was introduced in [19]. By relaxing the constraint to  $\mathcal{M}(\mathbf{z})$ , we propose a *surrogate* distribution with support everywhere in  $\mathbb{X}$ , but having maximum entropy among all distributions whose mean is constrained to  $\mathcal{M}(\mathbf{z})$ . We later argue that the probability mass of this surrogate distribution converges to  $\mathcal{M}(\mathbf{z})$ , anyway, and thereby converges (for large  $N$ ) to the idealized  $p_{x,0}(\mathbf{x}|\mathbf{z})$ .

### B. Surrogate Distribution

To approximate (5), we propose form (7), a proper distribution non-zero everywhere in  $\mathbb{X}$ . The surrogate distribution is given by substituting  $\boldsymbol{\alpha} = \mathbf{W}\mathbf{h}_z$  into (7): where  $\mathbf{h}_z$  is value of  $\mathbf{h}$  that solves

$$\mathbf{W}^T \lambda(\mathbf{W}\mathbf{h}) = \mathbf{z}, \quad (10)$$

and  $\lambda(\alpha, \alpha_0, \beta, \gamma)$  is the "activation function", which calculates the mean of  $p_e(x; \alpha, \alpha_0, \beta, \gamma)$ . For simplicity, we drop the dependence on  $\alpha_0, \beta, \gamma$ , which are taken from Table II.

We claim that  $p_s(\mathbf{x}; \mathbf{W}\mathbf{h}_z, \alpha_0, \beta, \gamma)$  approaches (5) asymptotically as  $N$  becomes large, i.e. the surrogate distribution converges to the posterior  $p_{0,x}(\mathbf{x}|\mathbf{z})$ , and so the mean of the surrogate distribution, given by

$$\bar{\mathbf{x}}_{\mathbf{z}} = \lambda(\mathbf{W}\mathbf{h}_z), \quad (11)$$

approaches the mean of  $p_{0,x}(\mathbf{x}|\mathbf{z})$ , and serves as the MaxEnt solution to the feature inversion problem. This convergence occurs quickly as a function of  $N$  (see Section IV.D and Fig. 8 in [19]).

The surrogate distribution mean  $\bar{\mathbf{x}}_z$  given by (11) enjoys numerous properties. It can also be shown that  $\mathbf{h}_z$  is the maximum likelihood estimate of  $\mathbf{h}$  under the likelihood function  $p(\mathbf{x}; \mathbf{h}) = p_s(\mathbf{x}; \mathbf{W}\mathbf{h}, \alpha_0, \beta, \gamma)$  [20]. As conditional mean estimator, it has well-known optimal properties including minimum mean square estimate (MMSE) [21]. In what follows, we demonstrate the usefulness of (11) in linear MaxEnt feature inversion.

Equations (10) and (11), together with Table I, form our unified approach to MaxEnt feature inversion. They can be used with a variety of data ranges and prior distributions, the most important of which appear in the table. Except in the unbounded data case (Gaussian prior), solving (10) requires an iterative algorithm [22].

#### IV. EXAMPLES

##### A. Unbounded Data

The unbounded problem  $\mathbb{X} = \mathbb{R}^N$  (Gaussian case) is solved in closed form using the well-known least-squares estimate

$$\bar{\mathbf{x}}_z = \mathbf{W} (\mathbf{W}^T \mathbf{W})^{-1} \mathbf{W}^T \mathbf{z} = \mathbf{W} (\mathbf{W}^T \mathbf{W})^{-1} \mathbf{z}, \quad (12)$$

which enjoys myriad optimality properties such as minimum mean square estimator, conditional mean, etc, and there is little to add to this. Equation (12) is also a solution to the idealized formulation (6). To see that our unified approach applies, using Table I, we see that  $\lambda(\alpha) = \alpha$ , so the solution  $\mathbf{h}$  to (10) is  $(\mathbf{W}^T \mathbf{W})^{-1} \mathbf{z}$ , and (12) follows.

##### B. Positive-Valued Data

The data range  $\mathbb{X} = \mathbb{P}^N$ , encompasses classical power spectral estimation [5], [10], [15], [16] and reconstruction of intensity images [6]–[10]. We seek a positive-valued vector  $\bar{\mathbf{x}}$  that meets linear constraint

$$\mathbf{W}^T \bar{\mathbf{x}} = \mathbf{z}. \quad (13)$$

The MaxEnt solution presented in [19] is vector  $\bar{\mathbf{x}}$ , that also meets

$$\sum_{i=1}^N \frac{B_{i,k}}{\bar{x}_i} = 0, \quad 1 \leq k \leq m, \quad (14)$$

where  $m = N - M$ , and  $\{B_{i,k}\}$  is the  $N \times (N - M)$  orthonormal matrix  $\mathbf{B}$  spanning the subspace orthogonal to the columns of  $\mathbf{W}$ .

This solution results by first seeking a probability distribution with highest entropy for positive-valued data with given mean  $\bar{\mathbf{x}}$ . This is the exponential distribution [13],

$$p(\mathbf{x}; \bar{\mathbf{x}}) \sim \prod_{i=1}^N \frac{1}{\bar{x}_i} \exp \left\{ -\frac{x_i}{\bar{x}_i} \right\}. \quad (15)$$

The entropy is then maximized subject to (13). Note that the entropy of (15) is given by [13]

$$H_e = \sum_{i=1}^N (1 + \log \bar{x}_i). \quad (16)$$

As an aside, note that maximizing (16) maximizes the spectral entropy (4), employed in power spectral estimation and sometimes in image reconstruction.

The entropy (16) under constraint (13) can go to infinity if, for example the unity vector  $\mathbf{1} = [1, 1 \dots 1]$  is orthogonal to the columns of  $\mathbf{W}$ . Then, the mean of  $\mathbf{x}$  can rise to infinity, together with the entropy. To avoid this, we assume that  $\mathbf{1} = \mathbf{W}\mathbf{u}$  for some vector  $\mathbf{u}$ . The two equations (13) and (14) provide  $N$  equations for the  $N$  unknowns, but can be solved only if there is at least one vector  $\mathbf{x} \in \mathbb{X}$  meeting (13).

We now check if our unified solution works in this case. By comparing (15) with (8), it can be verified that  $\lambda(\cdot)$  in Table I for exponential prior returns the distribution mean. Now substitute (11) into (10), and get  $\mathbf{W}^T \bar{\mathbf{x}}_z = \mathbf{z}$ , which meets (13). Furthermore, note that (14) states that the vector  $\bar{\mathbf{x}}^{-1} = [\frac{1}{\bar{x}_1}, \frac{1}{\bar{x}_2} \dots \frac{1}{\bar{x}_N}]$  is orthogonal to the columns of  $\mathbf{B}$ . But  $\bar{\mathbf{x}}^{-1} = -\alpha_0 - \alpha$ , where  $\alpha_0$  is the constant vector  $\alpha_0 = \alpha_0 \mathbf{1}$ . But  $\alpha_0$  is orthogonal to the columns of  $\mathbf{B}$  because we have assumed that  $\mathbf{1}$  is in the columns space of  $\mathbf{W}$ . Now,  $\alpha$  is the argument of  $\lambda(\cdot)$  in (10), so  $\alpha = \mathbf{W}\mathbf{h}$ . Therefore  $\alpha$  must also be orthogonal to  $\mathbf{B}$ , and (14) is met.

##### C. Doubly-Bounded Data

We now consider data with values to  $[0, 1]$ , such as found in digital photography. The solution has no classical equivalent and results in a novel entropy measure that was first reported in [19], Section V. The solution parallels the positive data case in the last section and is based on the truncated exponential distribution (TED), which is the maximum entropy distribution for data bounded to the interval  $[0, 1]$ , under mean (first moment) constraints ( see [23], page 186). The univariate TED distribution is provided in Table II with exponent parameter  $\alpha$  that can be positive or negative.

The MaxEnt solution is the vector  $\bar{\mathbf{x}}$  with elemental values in the range  $[0, 1]$  that meets (13) and

$$\sum_{i=1}^N \alpha_i B_{i,k} = 0, \quad 1 \leq k \leq m, \quad (17)$$

where the function  $\bar{x} = \lambda(\alpha)$  is taken from Table I for the TED case. Since  $\lambda(\alpha)$  is strictly monotonically increasing, there is a unique  $\bar{x}$  for each  $\alpha$ , so the  $N$ -dimensional vectors  $\bar{\mathbf{x}}$  and  $\alpha$  are equivalent parameterizations. This equation is similar to (14) in the positive data case, and we can make similar conclusions. Note that (17) is equivalent to the statement that the vector  $\alpha$  is in the column space of  $\mathbf{W}$ , or that there exists a free variable  $\mathbf{h}$  such that  $\alpha = \mathbf{W}\mathbf{h}$ . It is easy to verify the universal solution based on (10) and (11) with Tables I and II.

##### D. Additional Data Types and Non-Homogeneous Data

There are cases of interest where  $\mathbf{x}$  is non-homogeneous, having different range  $\mathbb{X}$  and MaxEnt prior distribution in each of the  $N$  elements, so that parameters  $\alpha_0, \beta, \gamma$ , and  $\mathbb{X}$  in Table II depend on the element index. Doing this poses no problem and does not affect the unified mathematical formulation. In addition to cases we already covered, the tables provide two distributions for the positive data case  $\mathbb{P}^N$ : the truncated

Gaussian (TG) and Chi-Squared(1) distributions. For  $\mathbb{P}^N$ , the TG distribution is MaxEnt for fixed variance and the Chi-Squared(1) distribution is MaxEnt when both the mean of  $x$  and the mean of  $\log(x)$  are specified (but they cannot be independently specified).

To demonstrate the use of non-homogeneous data, we passed a Gaussian noise vector of length  $N_f = 128$  into a filter, then computed the DFT, then the magnitude-squared of the DFT bins. This is non-homogeneous because the complex bins produce an exponential distribution, while the real bins result in Chi-sq(1). Next, we calculated the ACF up to an order of  $P = 6$  using the classical method: by taking the inverse DFT. We then set aside the first  $N = N_f/2 + 1$  magnitude-squared DFT bins as “unknown” input  $\mathbf{x}$ . Next, we formed the matrix  $\mathbf{W}$  to calculate the inverse DFT from  $\mathbf{x}$ , resulting in the length  $P + 1$  ACF. For this, we set

$$W_{i,k} = \frac{f(i)}{N_f^2} \cos\left(\frac{2\pi ik}{N_f}\right),$$

for  $i = 0, 1 \dots N - 1$ , and  $k = 0, 1 \dots P$ , where the function  $f(i) = 2$  when  $i = 0$  or  $i = N - 1$  and equals 1 otherwise. We verified that  $\mathbf{z} = \mathbf{W}^T \mathbf{x}$  indeed equals the ACF up to order  $P$ . We then created a bin-dependent function  $\lambda(\cdot)$  implementing the corresponding entries in Table I. We then solved equation (10) using an off-the shelf optimization program<sup>2</sup> for the variable  $\mathbf{h}$ . We then used (11) to compute  $\bar{\mathbf{x}}_z$ , the solution to the feature inversion problem.

For comparison purposes, we computed the classical autoregressive (AR) spectral estimate using Levinson algorithm, resulting in the AR spectrum  $p_{AR}(i) = N \left| \frac{e_0}{A_i} \right|^2$ , where  $e_0$  is the AR error variance, and where  $\{A_i\}$  are the DFT bins of the AR coefficients zero-padded to length  $N_f$ . The two spectral estimates,  $\bar{\mathbf{x}}_z$  and  $p_{AR}$ , agreed up to machine precision. This one example unifies distribution entropy (16), spectral entropy (4), and classical MaxEnt spectral estimation, using our unified approach using the nuances of the non-homogeneous bins.

### E. Auto-Encoder

For a modern example, we implemented feature inversion of intensity images with pixel values in  $[0, 1]$ , seen as a single-layer auto-encoder in machine learning terminology. Such a situation can also occur in intermediate network layers, after the use of *sigmoid* activation function and has been demonstrated in multiple-layer applications [22], [24]. Note also that this serves as an kind of optimal auto-encoder (in the sense of conditional mean) that does not require training, i.e. the reconstruction network is given, when the analysis network is known. We used a subset of the MNIST data set consisting of  $28 \times 28$  images of handwritten characters. Let  $\mathbf{x}$  be a  $n^2 \times 1$  vector reshaped from a square  $n \times n$  input image, where  $n = 28$ . The matrix  $\mathbf{W}$  is constructed to produce the 2-dimensional discrete cosine transform (DCT) from the input vector. In Figure 1, we show six examples. On the left-most column, the original images are shown. On the second column,

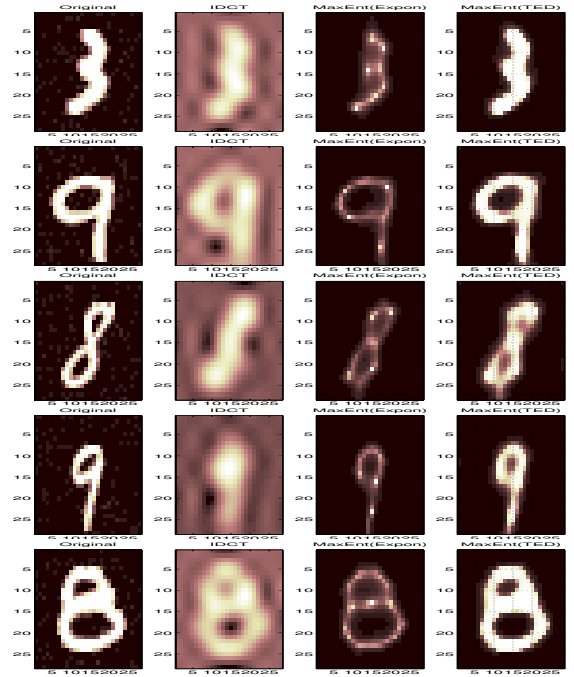


Fig. 1.  $28 \times 28$  images reconstructed from  $7 \times 7$  DCT features. Columns, from left to right: (a) Original, (b) reconstruction using inverse DCT, (c) MaxEnt reconstruction using **positive/Exponential** assumption, (d) MaxEnt reconstruction using **doubly-bounded/Uniform** assumption.

are shown the reconstructions using inverse DCT from the  $7 \times 7$  DCT coefficients, for a dimension reduction factor of 16. These images have negative values and values greater than 1, so are members of  $\mathbb{X}$ , and are very blurry, due to the large reduction in dimension. On the third column, we show the image reconstructed from the same DCT coefficients, using classical spectral entropy maximization assuming positive data. This is the formulation used by classical literature in image reconstruction [12]. There is a very noticeable but artificial improvement in sharpness. Due to the lack of an upper bound in intensity, we see a “glint” effect where some pixel values become large. Finally, we reconstructed the images using the doubly-bounded approach (uniform prior). These images are seen on the right-most column and look the most like the original images, preserving the original “fatness” of the handwritten characters.

### F. Conclusions

In this paper, we have provided a mathematical formulation for MaxEnt linear feature inversion that handles various data ranges and MaxEnt prior distributions with a single set of equations. We have verified that it works for known examples including classical image reconstruction and spectral estimation. In addition, we have provided an example of a new MaxEnt feature algorithm in an experiment that has modern applications, where data is constrained to  $[0, 1]$ . We demonstrated its superiority over classical image reconstruction, which does not take into account the upper bound.

<sup>2</sup>although it is better to use a Newton-Raphson algorithm that takes advantage of the known Hessian matrix.

## REFERENCES

- [1] E. T. Jaynes, "On the rationale of maximum-entropy methods," *Proceedings of IEEE*, vol. 70, no. 9, pp. 939–952, 1982.
- [2] A. Y. Khincin, *Mathematical Foundations of Information Theory*. Mineola, NY: Dover, 1957.
- [3] I. Csiszár, "Why least squares and maximum entropy? an axiomatic approach to inference for linear inverse problems," *The Annals of Statistics*, vol. 19, no. 4, pp. 2032–2066, 1991.
- [4] C. Nadeu, "Maximal flatness spectral modeling," *IEEE Transactions on Acoustics, Speech, and Signal Processing*, vol. 38, Nov 1990.
- [5] E. Reitsch, "The maximum entropy approach to inverse problems," *Geophysics*, vol. 42, pp. 489–506, 1977.
- [6] S. F. Gull and J. Skilling, "Maximum entropy method in image processing," *Proc. IEEE*, vol. 131, no. F(6), pp. 646–659, 1984.
- [7] R. Narayan and R. Nityananda, "Maximum entropy image restoration in astronomy," *Annual Review of Astronomy and Astrophysics*, vol. 24, pp. 127–170, 1986.
- [8] X. Zhuang, E. Østevold, and R. M. Haralick, "A differential equation approach to maximum entropy image reconstruction," *IEEE Trans ASSP*, vol. ASSP-35, pp. 208–218, Feb 1987.
- [9] X. Zhou, B. Li, Y. Zhang, H. Sun, and X. Lu, "A maximum entropy image reconstruction algorithm for 2-d synthetic aperture radiometers," in *Radar Conference, 2009 IET Internationals*, pp. 1–4, April 2009.
- [10] N. A. Malik, "One and two dimensional maximum entropy spectral estimation," *MIT PhD Thesis*, Nov 1981.
- [11] S. Kay, *Modern Spectral Estimation: Theory and Applications*. Prentice Hall, 1988.
- [12] S. J. Wernecke and L. R. D'Addario, "Maximum entropy image reconstruction," *IEEE Trans. Computers*, vol. C-26, no. 4, pp. 351–364, 1977.
- [13] J. N. Kapur, *Maximum Entropy Models in Science and Engineering*. Wiley (Eastern), 1993.
- [14] S. Geman and D. Geman, "Stochastic relaxation, Gibbs distributions, and the Bayesian restoration of images," *IEEE Transactions on Pattern Analysis and Machine Intelligence*, no. 6, p. 721741, 1984.
- [15] J. Burg. PhD thesis.
- [16] J. P. Burg, "The relationship between maximum entropy and maximum likelihood spectra," *Geophysics*, vol. 37, no. 2, pp. 375–376, 1971.
- [17] G. Wei and H. Zhen-Ya, "A new algorithm for maximum entropy image reconstruction," in *Proceedings of ICASSP-87*, vol. 12, pp. 595–597, April 1987.
- [18] P. M. Baggenstoss, "Maximum entropy PDF design using feature density constraints: Applications in signal processing," *IEEE Trans. Signal Processing*, vol. 63, June 2015.
- [19] P. M. Baggenstoss, "Uniform manifold sampling (UMS): Sampling the maximum entropy pdf," *IEEE Transactions on Signal Processing*, vol. 65, pp. 2455–2470, May 2017.
- [20] O. Barndorff-Nielsen and D. R. Cox, "Edgeworth and saddle-point approximations with statistical applications," *Journal of the Royal Statistical Society: Series B (Methodological)*, vol. 41, no. 3, pp. 279–299, 1979.
- [21] S. Kay, *Fundamentals of Statistical Signal Processing, Estimation Theory*. Prentice Hall, Upper Saddle River, New Jersey, USA, 1993.
- [22] P. M. Baggenstoss, "A neural network based on first principles," in *ICASSP 2020, Barcelona (virtual)*, (Barcelona, Spain), Sep 2020.
- [23] V. P. Singh, *Entropy, Theory and its Applications in Environmental and Water Engineering*. John Wiley & Sons, 2013.
- [24] P. M. Baggenstoss, "Applications of projected belief networks (pbn)," in *Proceedings of EUSIPCO 2019*, (La Coruña, Spain), Sep 2019.